Numerical Simulation Study on the Interaction of the Beam and Cavity Modes in an Inward-Emitting Coaxial Virtual Cathode Oscillator[*]

XING Qing-Zi[1;1)]   WANG Dong[1]   HE Xiao-Zhong[2]   ZHENG Shu-Xin[2]   DENG Jing-Kang[1]

1 (Department of Physics, Tsinghua University, Beijing 100084, China)
2 (Department of Engineering Physics, Tsinghua University, Beijing 100084, China)

Abstract The dominant frequency in an inward-emitting coaxial virtual cathode oscillator is solved analytically based on the steady-state relativistic-fluid-Maxwell equations. Full three-dimensional numerical simulation with the PIC method is carried out using the TS3 module of the MAFIA code. The frequency spectrum and the output power are obtained by monitoring the five propagating modes in the cylindrical output waveguide. The result shows that when the anode reflector exists, the frequency spectrum can be improved effectively by the formed quasi-cavity and hence the corresponding energy conversion efficiency can be enhanced.

Key words coaxial vircator, relativistic-fluid-Maxwell equations, MAFIA code, numerical simulation, high power microwave

1 Introduction

The inward-emitting coaxial vircator appears to be one of the most promising high-power microwave sources[1—8]. Fig. 1 demonstrates its typical structure. The electron beam, emitted by the cylindraceous cathode, moves along the radial direction and passes through the semi-permeable anode. When the beam current is higher than the space-charge-limited current of this region, an annular virtual cathode will be formed at a certain position between the anode and axis. Most of the electrons will be reflected by the virtual cathode and oscillate between the virtual and real cathode. Only a small portion of the electrons can penetrate the virtual cathode. The microwave emission is attributed to the energy exchange between the electrons and the electromagnetic field induced by the oscillation of the reflected electrons, and the oscillation of the position and potential of

the virtual cathode. Because the charge density increases as the radius decreases, the virtual cathode is produced more easily under the condition of low emitting current density. As a result, the damage on both the cathode and anode is decreased for the uniform electron beam with low density, which is especially important for a long pulse or the repetitive operation. In addition, the frequency spectrum can be improved by the quasi-cavity formed in the coaxial vircator[1, 2].
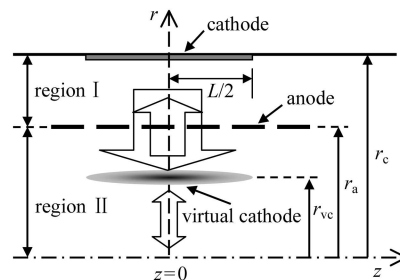

Fig. 1. Schematic diagram of the inward-emitting coaxial vircator.

The physical process of the interaction of the beam and cavity modes should be carefully considered and the quasi-cavity should be designed reasonably to obtain higher energy conversion efficiency.

Generally, there exists a central frequency for the dominant microwave power in the experiment of the vircator. A one-dimensional (1D) analytical model can give the estimated value of the oscillation frequency[1]. But the electron flow exhibits two-dimensional (2D) features in most experiments, which makes the 2D theoretical analysis necessary. 2D problems have been solved by W. Woo only for the planar vircator[9]. In Woo's work, the electrons are treated by the steady-state relativistic-fluid-Maxwell equations, and the frequency solution predicts the measured values within 20%. In this paper, the framework of Woo is extended to study the inward-emitting coaxial vircator. It is found for the first time that the dominant frequency can be solved through Eqs. (11) and (12). The comparison is made between the numerical solution and the simulation and experiment results.

A full three-dimensional (3D) numerical simulation code is needed to study the microwave frequency spectrum, which contains the azimuthally nonsymmetrical modes, and the physical process of the interaction of the beam and cavity modes in the inward-emitting coaxial vircator. The MAFIA module TS3, which is a 3D Particle-In-Cell (PIC) code, can calculate the time integration of the electromagnetic fields in a self-consistent way with the equations of motion of the charged particles. It has been applied to the 3D numerical simulation of the microwave tube electron gun[10] and the gyro-TWT. In this paper, the TS3 module of the MAFIA code is applied to the simulation study of the inward-emitting coaxial vircator for the first time. The frequency spectrum and the output power can be obtained by monitoring the propagating modes in the output waveguide.

2　Theoretical analysis

The method applied to the planar vircator[9] is extended to study the coaxial vircator in this sec-

tion. Being introduced the vector potential $\boldsymbol{A}$ and scalar potential ϕ, the steady-state relativistic-fluid-Maxwell equations can be described as

$$(\boldsymbol{u}\cdot\nabla)\boldsymbol{p}+e(\boldsymbol{E}+\boldsymbol{u}\times\boldsymbol{B})+(\nabla\cdot P_{\mathrm{t}})/n=0, \quad (1)$$

$$\nabla\times\boldsymbol{B}=-\mu_0 ne\boldsymbol{u}, \quad (2)$$

$$\boldsymbol{B}=\nabla\times\boldsymbol{A}, \quad (3)$$

$$\nabla\cdot\varepsilon_0\boldsymbol{E}=-ne, \quad (4)$$

$$\boldsymbol{E}=-\nabla\phi, \quad (5)$$

where P_{t} is the pressure tensor, n the electron density, μ_0 the vacuum permeability, ε_0 the vacuum permittivity, e the unit charge, and $\boldsymbol{u}$ and $\boldsymbol{p}$ the mean velocity and momentum of the electrons.

The diode current can be acquired by solving Eqs. (1)—(3)[11]. Following we will derive the equations of the dominant frequency from Eqs. (4) and (5) in the 2D axial-symmetric coordinate system. The equation of the electron's relativistic factor γ can be written as

$$\gamma(\boldsymbol{r})=1+e\phi(\boldsymbol{r})/mc^2. \quad (6)$$

Considering that the dominant frequency f is equal to the relativistic plasma frequency f_{p}, which is a constant in the space (or slowly varying in time), from

$$\omega_{\mathrm{p}}=2\pi f_{\mathrm{p}}=\sqrt{ne^2/(\gamma m\varepsilon_0)} \quad (7)$$

and Eqs. (4)—(6) we can get the equation of γ as

$$\nabla^2\gamma=(\omega_{\mathrm{p}}^2/c^2)\gamma. \quad (8)$$

The solution of Eq. (8) in region I is

$$\gamma=\mathrm{e}^{\pm kz}\cdot[A\cdot I_0(\alpha r)+B\cdot K_0(\alpha r)], \quad (9)$$

where I_0 and K_0 are the first and second kinds of the modified Bessel function. $\alpha^2+\kappa^2=\omega_{\mathrm{p}}^2/c^2$, where α and κ are the constants, describes the transverse and longitudinal motion of the electron. A and B are the dimensionless coefficients determined by the two boundary conditions: on the cathode surface the radial electric field and initial velocity of the electron are zero. Therefore the coefficients are

$$\begin{cases} A=1/[I_0(\alpha r_{\mathrm{c}})+I_1(\alpha r_{\mathrm{c}})K_0(\alpha r_{\mathrm{c}})/K_1(\alpha r_{\mathrm{c}})] \\ B=1/[K_0(\alpha r_{\mathrm{c}})+K_1(\alpha r_{\mathrm{c}})I_0(\alpha r_{\mathrm{c}})/I_1(\alpha r_{\mathrm{c}})] \end{cases}. \quad (10)$$

At the anode, we have $\gamma_0 = 1 + eV_0/mc^2$, where V_0 is the diode voltage. Substituting it into Eq. (9), we can get

$$\frac{I_0(\alpha r_a)}{I_0(\alpha r_c) + I_1(\alpha r_c)K_0(\alpha r_c)/K_1(\alpha r_c)} + \frac{K_0(\alpha r_a)}{K_0(\alpha r_c) + K_1(\alpha r_c)I_0(\alpha r_c)/I_1(\alpha r_c)} = \gamma_0, \quad (11)$$

where α can be obtained numerically. If the longitudinal motion of the electron is substantial, we can get $\alpha \gg \kappa$ at the dominant microwave emission. The dominant frequency becomes

$$f = \omega_p/2\pi \simeq c\alpha/2\pi. \quad (12)$$

For low voltages, Eqs. (11) and (12) reduce to the non-relativistic solution:

$$f \approx 9.44 \times 10^4 \cdot \frac{(r_a/r_c)^{1/4}}{(r_c - r_a)} V_0^{1/2}. \quad (13)$$

Another series approximation for $\alpha \cdot r_a > 1$ can be obtained from Eqs. (11) and (12) by expanding the Bessel functions in their series forms:

$$f = \frac{4.77 \times 10^7}{(r_c - r_a)} \ln\left[\sqrt{\frac{r_a}{r_c}}\gamma_0 + \left(\frac{r_a}{r_c}\gamma_0^2 - 1\right)^{1/2}\right]. \quad (14)$$

The non-relativistic solution agrees well with the numerical one for $V_0 \leqslant 0.5\text{MV}$. For higher voltages the series approximation becomes more applicable. Comparison of the observed and calculated dominant frequencies is shown in Fig. 2 for various reported experiments[2, 3] and simulations[4—7]. The numerical solution predicts the measured and simulated dominant frequencies within 10%.
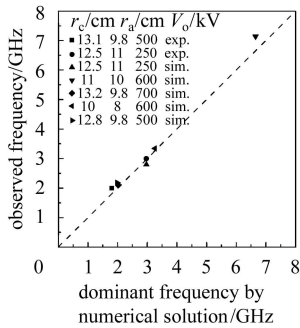

Fig. 2. Comparison of the observed and calculated dominant frequencies in the inward-emitting coaxial vircators for various reported experiments[2, 3] and computer simulations[4—7].

The dominant frequencies in the planar vircator

derived from the 1D[12] and 2D theories[9] are same:

$$f = \frac{4.77 \times 10^7}{d} \ln[\gamma_0 + (\gamma_0^2 - 1)^{1/2}], \quad (15)$$

where d is the anode-cathode gap distance. Eq. (15) has been applied to the coaxial vircators[13] and can also predict the dominant frequency within 10% for the parameters in Fig. 2. Our analysis gives the theoretical support to it. When $r_a/r_c \sim 1$, the series approximation (Eq. (14)) becomes the same as Eq. (15). It reveals that if the anode-cathode gap d is relatively small compared to the cathode radius, the dominant frequency in a coaxial vircator is similar to that produced by a planar vircator with the same d.

Eq. (11) and (12) are derived from the coaxial structure and can replace Eq. (15) to estimate the dominant frequency for the coaxial vircator. It is more applicable for relatively larger anode-cathode gaps.

3　Numerical simulation

The 3D PIC code, TS3 module of MAFIA, is adopted to study the physical interaction of the beam and cavity modes in the inward-emitting coaxial vircator. A computer model is established and shown in Fig. 3. The main parameters are from Ref. [2], with $r_c=7\text{cm}$, $r_a=5.5\text{cm}$, $V_0=250\text{kV}$, the radius of the cylindrical waveguide $r_w=5.5\text{cm}$, the diode current of 20kA, the pulse length of 20ns, the width of the cathode emission region of 3cm, and the distance between the cathode and anode reflector of 5cm. An xyz coordinate system is adopted for the sake of using the waveguide boundary condition. The number of the mesh points and macroparticles are 2×10^6 and 1×10^6, respectively.
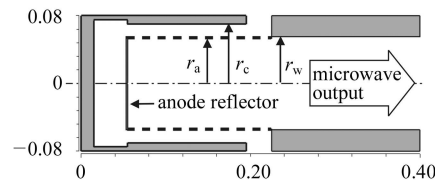

Fig. 3. The computer model established by MAFIA code.

The potential distribution between the anode and axis is altered due to the space charge effect of the electron beam. It decreases as the current becomes

larger, until the minimum potential in that region reaches the value that equals the potential of the cathode. The virtual cathode evolves at the position with the minimum potential. Fig. 4 gives the transverse phase space $P_r \sim r$ of the beam at $t=16$ns obtained by MAFIA, which shows the evidence of the virtual cathode evolution near $r=4$cm. From Fig. 4 the motion of the electron beam in the coaxial vircator can be distinguished clearly. The electrons are accelerated in the diode after emission, decelerated before they reach the virtual cathode, accelerated from the virtual cathode to the anode, and decelerated after they return the diode region.
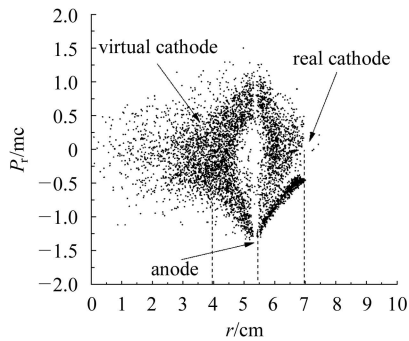

Fig. 4. Transverse phase space of the beam ($t=16$ns).

The cylindrical waveguide port should be defined as the waveguide boundary in the M module to monitor the microwave output. All parts of the 3D-field not consisting of waveguide modes, which have been defined, will be reflected at the boundary planes. The propagating modes can be calculated in the E module. The dominant frequency estimated from Eqs. (11) and (12) is near 3GHz. As shown in Fig. 5, five propagating modes are found by the E module, where TE11 and TE21 modes have two degenerated modes, respectively. The relative error of the longitudinal propagation constants (as shown in Table 1) given by MAFIA is less than 1% compared with the theoretical values.

Table 1. The lowest five propagating modes in the cylindrical waveguide ($r_w=5.5$cm, $f=3$GHz).

modes	cut-off freq./ GHz	longitudinal propagation constant/m^{-1}
TE11_A/ TE11_B	1.60	53.1
TM01	2.09	44.8
TE21_A/ TE21_B	2.65	29.2

(a) TE11_A   (b) TE11_B   (c) TM01

(d) TE21_A   (e) TE21_B
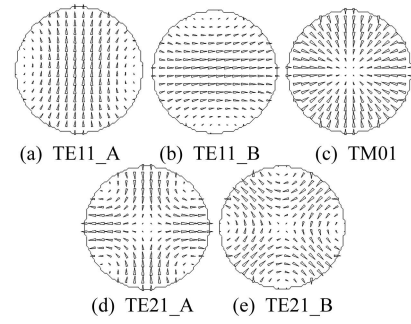
Fig. 5. Field distribution of the propagating modes in the cylindrical waveguide given by MAFIA E module($r_w=5.5$cm, $f=3$GHz, (a) and (b), (d) and (e) are degenerated modes).
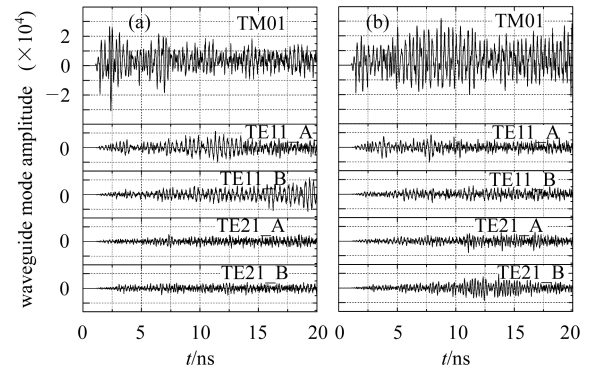

Fig. 6. Waveguide mode amplitude for the propagating modes.
(a) Without the anode reflector; (b) With the anode reflector.

All the five modes are loaded to the cylindrical waveguide port in the TS3 module. Thus the 3D-field of these modes can be transmitted through the port without reflection. Because the structure of the coaxial vircator and electron distribution are both axial-symmetric, the induced electromagnetic field is assumed to contain mainly the azimuthally symmetrical modes. For the present parameters, TM01 is considered to be the dominant mode. TM02 is not concerned because its cut-off frequency (4.79GHz) is much larger than 3GHz. The waveguide mode amplitude (namely the normalized voltage) at the port is monitored for the five modes with and without the anode reflector, as shown in Fig. 6. The frequency spectra are acquired by FFT transformation, as shown in Fig. 7. The result shows that, the voltage amplitude of TM01 is the largest for the two situations. The azimuthally nonsymmetrical modes, TE11 and TE21, have much less amplitudes. Due to the formed quasi-cavity, the dominant frequency component is more

apparent when the anode reflector exists. The dominant frequency given by Fig. 7(b) is 3.03GHz, which agrees well with the numerical solution of Eqs. (11) and (12).
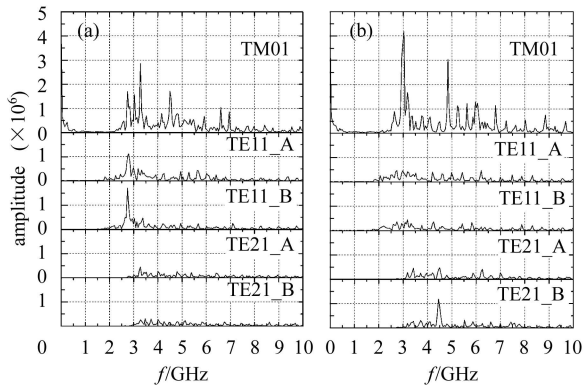

Fig. 7. FFT transformation of the waveguide mode amplitude.
(a) Without the anode reflector; (b) With the anode reflector.
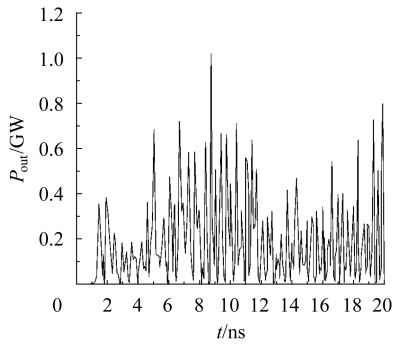

Fig. 8. Instantaneous microwave power at the output port as a function of time for TM01 mode.

The instantaneous microwave power can be obtained from the envelope of the square of the normalized voltage at the waveguide port. The output power for each mode can be derived by integrating and averaging its instantaneous power separately. The instantaneous power at the output port as a function of time is shown in Fig. 8 for TM01 mode when the anode reflector exists. The corresponding power is 191MW. The output power of the five modes is shown in Table 2. The total microwave power can be estimated by adding the power of the modes, which is 226MW with the anode reflector and 141MW without the anode reflector. The corresponding energy efficiency is 4.5% and 2.8%, respectively. It can be drawn that with the anode reflector the azimuthally nonsymmet-

rical modes are restrained, and the frequency spectrum is improved due to the formed quasi-cavity. As a result, higher energy efficiency is achieved in the coaxial vircator.

Table 2. Output power for the propagating modes.

propagating mode	output power/MW (without the anode reflector)	output power/MW (with the anode reflector)
TE11_A	16	11
TE11_B	16	7
TM01	100	191
TE21_A	5	6
TE21_B	4	11
total power/MW	141	226

The dominant frequency and total output power obtained by the numerical simulation are compared with the analytic solution and reported experiment[2], as shown in Table 3. The dominant frequency given by MAFIA is consistent with the experiment, and the total power agrees in magnitude. Though there is simplicity in the simulation model, satisfactory result has been given by MAFIA TS3 module.

Table 3. Comparison of the simulation result with the analytic solution and experiment[2].

	dominant frequency/GHz	output power/MW
analytic solution	2.92	
MAFIA	3.03	226
experiment	2.89	230

4 Conclusions

To enhance the energy efficiency of the inward-emitting coaxial vircator, one should carefully design its quasi-cavity to obtain the desired dominant frequency and narrow bandwidth. The dominant frequency can be numerically solved with Eqs. (11) and (12), which are derived from the steady-state relativistic-fluid-Maxwell equations. Through numerical simulation carried out with the MAFIA TS3 module, the frequency spectrum and output power can be obtained by monitoring the propagating modes in the output waveguide. The result shows that TM01 is the dominant mode, and the azimuthally nonsymmetrical modes (TE11 and TE21) have relatively less intensity. When the anode reflector exists, the dominant frequency component is more

apparent due to the formed quasi-cavity. At the same time, TE11 and TE21 modes are restrained, and the frequency spectrum is improved. As a result, higher energy efficiency is achieved.

To further enhance the energy efficiency, the optimization of the cathode emission region and the distance between the cathode and anode reflector is in process.

The authors would like to thank SHAO Hao for valuable suggestions and discussions.

References

1 JIANG W, Woolverton K, Dickens J et al. IEEE Trans. Plasma Sci., 1999, **27**(5): 1538—1542

2 SHAO H, LIU G Z, YANG Z F. Preliminary Experimental Study of Novel Coaxial Virtual Cathode Oscillator(Vircator). Proc. 5th HPM Conf. China. Zhuhai: 2002. 263—267 (in Chinese)
(邵浩, 刘国治, 杨占峰. 同轴虚阴极振荡器初步实验研究. 第五届全国HPM会议论文集. 珠海: 2002. 263—267)

3 JIANG W, Dickens J, Kristiansen M. IEEE Trans. Plasma Sci., 1999, **27**(5): 1543—1544

4 SHAO H, LIU G Z, SONG Z M et al. Numerical Simulation Studies of Coaxial Vircators. Proc. 12th Inter. Conf. High-Power Particle Beams. Piscataway: IEEE Press, 1998. 792—795

5 CHEN X D, Toh W K, Lindsay P A. IEEE Trans. Plasma Sci., 2004, **32**(3): 1191—1199

6 YANG W Y, DING W. IEEE Trans. Plasma Sci., 2004, **32**(3): 1187—1190

7 XIE W K, XIAO S L, QIAN G D. J. UEST of China, 1999, **28**(2): 166—170 (in Chinese)
(谢文楷, 肖顺禄, 钱光第. 电子科技大学学报, 1999, **28**(2): 166—170)

8 Sung K Y, Jeon W, Jung Y et al. IEEE Trans. Plasma Sci., 2005, **33**(4): 1353—1357

9 Woo W. Phys. Fluids, 1987, **30**(1): 239—244

10 LIAO P, YANG Z H, LEI W Q et al. High Power Laser and Particle Beams, 2004, **16**(3): 353—357 (in Chinese)
(廖平, 杨中海, 雷文强等. 强激光与粒子束, 2004, **16**(3): 353—357)

11 XING Q Z, WANG D, HUANG F et al. IEEE Trans. Plasma Sci., 2005, accepted

12 Hwang C S, WU M W, SONG P S et al. J. Appl. Phys., 1991, **69**(3): 1247—1252

13 Crawford M, Kristiansen M, Hatfield L L. Experimental Results from a Coaxial Virtual Cathode Oscillator. IEEE Int. Conf. Pulsed Power. Albuquerque: IEEE Press, 1995. 682—687

向内发射同轴虚阴极振荡器波束互作用的数值模拟研究*

邢庆子[1;1)] 王冬[1] 何小中[2] 郑曙昕[2] 邓景康[1]

1 (清华大学物理系 北京 100084)
2 (清华大学工程物理系 北京 100084)

摘要 对向内发射同轴虚阴极振荡器微波主频进行了解析求解, 利用稳态相对论流体Maxwell方程组得到了微波主频所满足的方程; 同时使用MAFIA程序的TS3模块对向内发射同轴虚阴极振荡器中波束互作用进行了全三维PIC数值模拟研究, 通过对微波输出圆波导中5个传输模式的监测, 得到了各模式的频谱分布及输出功率. 结果表明, 在有阳极反射板存在时, 构成的准腔结构能够有效地改善频谱, 从而提高能量转换效率.

关键词 同轴虚阴极振荡器 相对论流体Maxwell方程组 MAFIA程序 数值模拟 高功率微波